

1 **Metagenomic analysis of a blood stain from the French revolutionary Jean-Paul Marat (1743-** 2 **1793)**

3
4 Toni de-Dios^{1*}, Lucy van Dorp^{2**}, Philippe Charlier^{3*}, Sofia Morfopoulou^{2,4}, Esther Lizano¹,
5 Celine Bon⁵, Corinne Le Bitouzé⁶, Marina Álvarez-Estapé¹, Tomas Marquès-Bonet^{1,7,8,9}, François
6 Balloux²⁺, Carles Lalueza-Fox¹⁺

7
8 ¹Institute of Evolutionary Biology (CSIC-Universitat Pompeu Fabra), 08003 Barcelona, Spain

9 ²UCL Genetics Institute, University College London, London WC1E 6BT, UK

10 ³Département de la Recherche et de l'Enseignement, Musée du Quai Branly - Jacques Chirac,
11 75007 Paris, France

12 ⁴Division of Infection and Immunity, University College London, London WC1E 6BT, UK

13 ⁵Département Hommes, Natures, Sociétés, Muséum National d'Histoire Naturelle, 75116 Paris,
14 France

15 ⁶Archives Nationales, 75004 Paris, France

16 ⁷Catalan Institution of Research and Advanced Studies (ICREA), 08010 Barcelona, Spain

17 ⁸CNAG-CRG, Centre for Genomic Regulation, Barcelona Institute of Science and Technology
18 (BIST), 08036 Barcelona, Spain

19 ⁹Institut Català de Paleontologia Miquel Crusafont, Universitat Autònoma de Barcelona, 08193
20 Cerdanyola del Vallès, Barcelona, Spain

21
22 *These authors equally contributed to this work

23 + Co-corresponding authors

24 25 **Significance**

26
27 The advent of second-generation sequencing technologies allows for the retrieval of ancient
28 genomes from long-dead people and, using non-human sequencing reads, of the pathogens that
29 infected them. In this work we combined both approaches to gain insights into the ancestry and
30 health of the controversial French revolutionary leader and physicist Jean-Paul Marat (1743-
31 1793). Specifically, we investigate the pathogens, which may have been the cause of the
32 debilitating skin condition that was affecting him, by analysing DNA obtained from a paper
33 stained with his blood at the time of his death. This allowed us to confidently rule out several
34 conditions that have been put forward. To our knowledge, this represents the oldest successful
35 retrieval of genetic material from cellulose paper.

36 37 **Abstract**

38
39 The French revolutionary Jean-Paul Marat was assassinated in 1793 in his bathtub, where he
40 was trying to find relief from the debilitating skin disease he was suffering from. At the time of
41 his death, Marat was annotating newspapers, which got stained with his blood and were
42 subsequently preserved by his sister. We extracted and sequenced DNA from the blood stain
43 and also from another section of the newspaper, which we used for comparison. Analysis of
44 human DNA sequences supported the heterogeneous ancestry of Marat, with his mother being
45 of French origin and his father born in Sardinia, although bearing more affinities to mainland
46 Italy or Spain. Metagenomic analyses of the non-human reads uncovered the presence of fungal,
47 bacterial and low levels of viral DNA. Relying on the presence/absence of microbial species in
48 the samples, we could confidently rule out several putative infectious agents that had been
49 previously hypothesised as the cause of his condition. Conversely, some of the detected species
50 are uncommon as environmental contaminants and may represent plausible infective agents.
51 Based on all the available evidence, we hypothesize that Marat may have suffered from a

52 primary fungal infection (seborrheic dermatitis), superinfected with bacterial opportunistic
53 pathogens.
54

55 Background

56

57 Jean-Paul Marat (1743-1793) was a famous French physician, scientist and journalist, best
58 known for his role as Jacobin leader during the French Revolution. Marat's parents were
59 Giovanni Mara, born in Cagliari, Sardinia, who later added a "t" to his family name to give it a
60 French feel and Louise Cabrol, a French Huguenot from Castres. Marat was stabbed to death in
61 his bathtub by the Girondist' supporter Charlotte Corday on July 13th, 1793 (Figure 1a). Upon his
62 death, his sister Charlotte Albertine kept two issues of Marat's newspaper *l'Ami du Peuple*
63 (n°506 and n°678, published on June 30th, 1791 and August 13th, 1792, respectively), which he
64 was annotating the day of his assassination and that got stained with his blood (Figure 1b).
65 Albertine gave the issues to the collector François-Nicolas Maurin (1765-1848) in 1837. After his
66 death, as explained by a handwritten note by writer Anatole France dated from October 10th,
67 1864, the two issues ended up in the possession of baron Carl De Vinck who in 1906 donated
68 them to the Département des Estampes, Bibliothèque National de France, in Paris (see notice in
69 the Catalogue Général: <https://catalogue.bnf.fr/ark:/12148/cb40261215w>).

70

71 Marat's health during the last years before his assassination is shrouded in mystery. He suffered
72 from a severe itching skin disease from which he found some relief by spending most of his time
73 in a medicinal bathtub over which he placed a board to use as a writing desk. His condition,
74 which he attributed to his stay in the sewers of Paris while hiding from his political enemies, has
75 been the subject of numerous medical debates and has been alternatively attributed to scabies,
76 syphilis, atopic eczema, seborrheic dermatitis or dermatitis herpetiformis (1–5), the latter as a
77 potential manifestation of celiac disease (6). It has been suggested that his condition affected
78 his character and turned it more violent (1).

79

80 With the intention of shedding light on these issues, we retrieved two samples from one of the
81 newspapers stained with Marat's blood, one sample from the blood stain and a second one from
82 a non-stained area in the upper corner of the paper, to be used as a comparison. A principal
83 concern was to use a non-destructive approach to explore Marat's genomic footprint; therefore,
84 the samples were taken with forensic swabs. The DNA extracted from both samples was used to
85 build genomic libraries that were subjected to second-generation sequencing using the Illumina
86 platform. DNA reads were subsequently classified, separating the human reads – most likely
87 deriving from Marat's blood – from those assigned to microbial species. The analysis of both sets
88 of DNA sequences allowed characterisation of Marat's ancestry as well as identification of the
89 potential pathogens responsible for his debilitating skin condition.

90 Results

91

92 Human ancestry analysis

93

94 We generated 568,623,176 DNA reads from the blood stain, of which 74,244,610 reads mapped
95 to the human reference genome (Table S1). From these, we retrieved a complete human
96 mitochondrial (mtDNA) genome at a mean depth of coverage of 4.038x and the nuclear genome
97 at 0.029x (Table S1). The predominant mtDNA haplotype was H2a2a1f, although we found
98 evidence of some additional mtDNA sequences, notably a K1a15 haplotype. The ratio of sexual
99 chromosome to autosomal DNA reads indicated that the sample donor was male (Fig. S1).

100

101 The human DNA reads showed evidence of post-mortem deamination occurring in 1% of the
102 ends of sequencing reads, indicating authentic ancient DNA damage (Fig. S2). For further
103 analyses we selected only those reads that displayed C to T or G to A substitutions at the 5' or 3'
104 end, respectively. After this procedure, the degree of mitochondrial contamination was reduced
105 to 0-0.01%.

106

107 To explore the ancestry of Marat in the context of modern European populations, we performed
108 Principal Component Analysis (PCA) (Figure 2a and Fig. S3) and unsupervised clustering in
109 ADMIXTURE (Figure 2b). Our sample projected among modern French individuals sampled from
110 "Southern" France in the population genetic analyses. This result is broadly compatible with the
111 mixed ancestry of Marat, especially if his paternal family was not Sardinian native but
112 descendant of recent Italian or Spanish immigrants, as has been speculated (2). However, mixed
113 ancestries are difficult to discern, especially when only limited genetic data is available.

114

115 Metagenomic analysis

116

117 We conducted metagenomic species assignments with the 9,788,947 deduplicated, quality
118 controlled and low complexity filtered DNA reads (combined merged and non-merged) that did
119 not map to the human genome (see Methods and Table S2). We used metaMix (7), a Bayesian
120 mixture model framework developed to resolve complex metagenomic mixtures, which
121 classified ~9% of the non-human reads into 1,328 microbial species (Table S3). The species
122 assignments were replicated with KrakenUniq (8), which led to largely consistent, if less
123 accurate, results (~7% classified into 3,213 species, Fig. S4, Table S4). Thus, we relied on the
124 metaMix species assignments throughout the paper, unless stated otherwise.

125

126 We detected the presence of a wide range of microorganisms, including some expected to
127 develop on decaying cellulose and/or dried blood, but also others recognized as opportunistic
128 human pathogens from the following bacterial genera: *Acidovorax*, *Acinetobacter*, *Burkholderia*,
129 *Chryseobacterium*, *Corynebacterium*, *Cutibacterium*, *Micrococcus*, *Moraxella*, *Paraburkholderia*,
130 *Paracoccus*, *Pseudomonas*, *Rothia*, *Staphylococcus*, *Streptococcus* and the fungal genera
131 *Aspergillus*, *Penicillium*, *Talaromyces* and *Malassezia* as well as HPV (type 179 and type 5) and
132 HHV6B viruses, albeit the latter supported by a very low numbers of reads (Table S3, S4). Some
133 of the DNA reads, notably from *Aspergillus glaucus*, *Cutibacterium acnes*, *Malassezia restricta*
134 and *Staphylococcus epidermis* showed typical misincorporation patterns that are considered
135 indicative of these sequences being authentically old (Fig. S5).

136

137 We additionally sequenced the swab taken from the unstained paper sample. In this case, only
138 96,252 paired DNA sequencing reads were obtained (56,616 merged, 25,712 non-merged,
139 36,434 deduplicated combined merged and non-merged), with 52% of the reads that could be
140 classified with metaMix into 64 species and 36% with KrakenUniq into 953 species, respectively
141 (see Methods and Table S3). Although very little DNA could be retrieved from the section of the

142 document that had not been blood-stained, we tried to identify microorganisms that were
143 statistically over-represented in the blood stain relative to the unstained paper. Amongst these
144 and besides, as expected, *Homo sapiens*, different species of *Aspergillus* and *Acinetobacter* were
145 significantly overrepresented in the blood stain (Table S3). It remains questionable however
146 whether the unstained paper represents a suitable negative control given that the newspaper
147 had been extensively manipulated by Marat. Significant over-representation of *Aspergillus spp.*
148 and *Acinetobacter spp.* in the blood stain relative to the rest of the document could also be due
149 to the blood providing better conditions for the growth of iron-limited microbes. Indeed,
150 *Aspergillus spp.* and *Acinetobacter spp.* are commonly found in the environment but are also
151 grown in blood agar. As such, it is plausible that these represent *post-mortem* contaminants.
152 Indeed, for *Acinetobacter spp.* we identified no post-mortem damage pattern.

153
154 Metagenomic analysis of historical samples can be challenging as the resulting microbial
155 communities typically comprise an unknown mixture of endogenous species as well as
156 contaminants, both contemporary and modern. As such, we relied on a differential diagnostics
157 approach (Table 1), where we specifically tested for the presence of reads from pathogens that
158 could plausibly have led to Marat's symptoms, most of which have been previously hypothesised
159 in the literature (1–5).

160
161 Based on the absence of any sequencing reads in either the blood stain or the unstained paper
162 we could rule out syphilis, leprosy, scrofula (tuberculosis) and diabetic candidiasis (thrush)
163 (Table 1, Table S3). We additionally tested for scabies, which is caused by burrowing of the mite
164 *Sarcoptes scabiei* under the skin. Since the metagenomic reference database did not include
165 arthropod genomes, this was tested separately by blasting all the non-human reads against the
166 *Sarcoptes scabiei* genome (GCA_000828355.1). Again, we detected not a single read matching
167 to *Sarcoptes scabiei*, which also allowed ruling out scabies out as the cause of Marat's skin
168 disease (Table 1, Table S3).

169
170 Conversely, metaMix recovered 15,926 and 83 filtered DNA reads from the blood stain and the
171 unstained paper respectively, assigned to *Malassezia restricta* a fungal pathogen causing
172 seborrheic dermatitis, which has been previously hypothesized as one of the most plausible
173 causes for Marat's condition (1–4). Direct mapping of all reads to *M. restricta*
174 (GCA_003290485.1) resulted in 19,194 reads from the blood stain dataset mapping over 17.17%
175 of the reference genome. KrakenUniq failed to identify *M. restricta*, instead assigning 627 reads
176 sequenced from the blood stain to *M. sympodialis*. However, further analysis of the *Malassezia*
177 reads based on genome mapping pointed to most (80.3%) being uniquely assigned to *M.*
178 *restricta* rather than *M. sympodialis* (Fig. S6). This allowed us to reconstruct a complete *M.*
179 *restricta* mtDNA genome at 0.84X coverage. The *Malassezia* reads were evenly distributed along
180 the full genome supporting no mixing or misclassification of the species (Fig. S7). We placed our
181 Marat *M. restricta* genome in phylogenetic context by building a maximum likelihood phylogeny
182 including our historical strain and available present-day mtDNA *M. restricta* genomes. Although
183 the total number of samples is small, the fact that the *M. restricta* mtDNA molecule recovered
184 from Marat's blood is placed basal to modern strains (Fig. S8) and exhibits some post-mortem
185 damage (Fig. S5) further support its authenticity.

186
187 We also recovered 587 filtered reads assigned by metaMix to *Staphylococcus aureus* in the blood
188 stain but none in the reads obtained from the unstained paper. The differential representation
189 in the two samples is not significantly different due to the far lower number of reads in the
190 unstained sample (Table S3). *S. aureus* is a common human pathogen and the leading cause of
191 atopic eczema. In order to confirm the metagenomic assignments to *S. aureus*, we mapped the
192 raw microbial reads to a series of reference genomes from various species in the *Staphylococcus*
193 genus. This allowed us to identify 888 reads mapping against the *S. aureus* reference genome,

194 out of which 758 uniquely mapped to *S. aureus* (Fig. S9). The relatively low number of reads may
195 point to a secondary infection by *S. aureus* rather than *S. aureus* being the initial cause of Marat's
196 condition.

197
198 The most prevalent microbial species in the blood stain was *Cutibacterium acnes*
199 (formerly *Propionibacterium acnes* (9)), which was also present in the unstained paper (Table
200 S3). *C. acnes* is largely a commensal and part of the normal skin biota present on most healthy
201 adult humans' skin, including in association with *S. epidermis* which we also observe in our
202 sample (Table S3, Table S4, Fig. S10) (10). *C. acnes* is also a frequent contaminant in
203 metagenomic samples (11, 12). However, *C. acnes* is also involved in severe acneiform eruptions
204 (13) and could have contributed to Marat's condition. 86,019 reads mapped to the *C. acnes*
205 reference genome (GCF_000008345.1), yielding an alignment of 3.4X average coverage (Fig.
206 S10) and exhibiting moderate post-mortem damage (Fig. S5).

207
208 A phylogeny of Marat *C. acnes* with a collection of publicly available modern strains (12, 14)
209 places our historic genome on a short branch falling basal to Type I strains, supporting its age
210 and authenticity (Fig. S11). This phylogenetic placement suggests our Marat strain falls into *C.*
211 *acnes* phylotype I (*C. acnes subsp. acnes*) rather than II (*C. acnes subsp. defendens*). Whilst our
212 Marat strain does not cluster with phylotype Ia, the type more commonly associated with skin
213 surface associated acne vulgaris (15), its position, basal to Type Ib strains could be consistent
214 with soft or deep tissue infections, with associated haemolytic activity (16).

215 Discussion

216

217 Over the last decade, ancient-pathogen genomics has made great progress by borrowing
218 technological advances originally developed for the study of human ancient DNA (17, 18).
219 Although most microbial data has been secondarily generated from the sequencing of ancient
220 human bones or teeth (18–21) other, rare samples, such as preserved tissues (22, 23) or
221 microscope slides from antique medical collections have been analysed (17, 24). We are aware
222 of no previous attempt to leverage ancient DNA technology to diagnose infections in historical
223 characters, despite previous sequencing of remains from other prominent historical figures such
224 as King Richard III and the putative blood of Louis XVI (25, 26).

225

226 In this work we analysed both human and ‘off-target’ microbial reads to shed light on an
227 important historical figure of the French Revolution and his skin condition. Due to the loss of
228 Marat’s remains after their removal from the Panthéon in February 1795, the paper stained with
229 his blood likely represents the only available biological material to study both his ancestry and
230 the cause of his skin condition. Our work also represents the first instance where second-
231 generation sequencing techniques have been applied to old cellulose paper.

232

233 The presence and relative abundance of different microorganisms in the documents Marat was
234 annotating is affected by their endogenous presence as well as contemporary and modern
235 contamination both for the blood and unstained sample. Some microorganisms present in the
236 samples might reflect skin microbiome signatures. Whilst some other microorganisms represent
237 environmental contaminants and are likely unrelated to Marat’s condition. Nevertheless, we can
238 use classification of metagenomic samples to test some of the proposed diagnoses of Marat’s
239 condition (Table 1). For instance, due to the conspicuous absence of DNA reads from several
240 previously proposed pathogen candidates, we can confidently exclude syphilis, tuberculosis
241 (scrofula), leprosy, diabetic candidiasis or scabies as causative agents.

242

243 The presence of *Malassezia restricta* is intriguing because this fungus is specialized to live on the
244 skin (27). *Malassezia* has been described in various skin conditions, including dandruff, atopic
245 eczema, folliculitis and seborrheic dermatitis (28, 29). Interestingly, the latter symptoms would
246 fit those described in Marat (5). The *M. restricta* reads were not statistically significantly
247 overrepresented in the blood’s stain relative to the unstained paper, although they could be
248 expected to be present in both samples if someone heavily infected was holding the newspaper.
249 Though, the damage patterns and phylogenetic placement relative to modern samples of the
250 *M. restricta* mitochondrial genome assembled from the reads in Marat’s blood suggests they are
251 indeed old (Fig. S5, Fig. S8). Also of interest is the widespread presence of *Cutibacterium acnes*
252 *subsp. acnes*, causative of severe acneiform eruptions, which constitutes the top hit in the blood
253 sample and falls basal to phylotype I strains currently in circulation. *Staphylococcus aureus*,
254 which is frequently detected in cases of atopic dermatitis, is also present in reads obtained from
255 the blood’s stain, although in low number.

256

257 Whilst our results do not allow us to reach a definite diagnosis of Marat’s condition, they allowed
258 us to rule out several previous hypotheses and provide suggestive evidence that he could have
259 been suffering from an advanced polymicrobial infection, either primary or secondary to
260 another condition. Future metagenomic analysis of additional documents in Marat’s possession
261 during his assassination could help confirm the microbial composition found in this study and
262 strengthen these observations.

263

264 Our work further illustrates the potential of sequencing technologies for the generation of
265 (meta-)genomic information from difficult, singular samples and opens new avenues to address
266 medical hypotheses of major historical interest.

267 **Material and methods**

268

269 *DNA extraction and sequencing*

270 Forensic swabs were obtained from one of the newspapers Marat was annotating at the time of
271 his assassination. One swab was taken from the blood stain and another from an area of the
272 newspaper without visual evidence of blood. The blood swab was extracted with a buffer
273 composed of 10 mM TrisHCl, 10 mM EDTA, 2 mM SDS, 50 mM DTT; proteinase K was added after
274 one hour incubation. The extract was subsequently concentrated and purified using a Qiagen
275 column kit. DNA extraction from both swabs was performed together with extraction blanks (no
276 sample). A total of 35 ul of each sample was used for library preparation following the BEST
277 protocol (30). Libraries were quantified using BioAnalyzer and sequenced by HiSeq 4000
278 (Illumina). Library blanks were also performed for each library batch.

279

280 *Mapping and variant calling*

281 Raw sequences adapters were removed using *Cutadapt* (31). Reads were then aligned against
282 the Human Reference genome (GRCh37/hg19) and the mitochondrial reference genome (rCRS)
283 as well as for a set of microbial candidates using *BWA* v.07.3 (32) and *Bowtie2* (33). Duplicate
284 reads were discarded using *Picard* tools (34). Unique mapped reads were filtered for a mapping
285 quality equal of above 30. All mapped sequences (human and microbial) were assessed for post-
286 mortem damage patterns at the ends of reads using *MapDamage* v.2 (35), which can be used as
287 a sign of historic authenticity over modern contamination. Mapping statistics including the
288 depth of coverage were recorded using *Qualimap* (36). Due to the low coverage of the human
289 sample, we performed a pseudo-haploid calling approach, common to the processing of aDNA,
290 using the *SAMtools Pileup* tool (37). This data was then merged with the Human Origins dataset
291 for its use in population genetics analyses (38, 39).

292

293 *Modern DNA Contamination*

294 *Schmutzi* was used to estimate the amount of modern DNA contamination in the mitochondrial
295 (mtDNA) genome (40) likely deriving from the DNA of those who have handled the newspaper
296 in the years following Marat's death. This allowed the modern DNA sequences to be delineated
297 from the ancient DNA sequences using *Jvarkit* and a custom script (41) by selecting the human
298 reads with mismatches in their first or last three nucleotides. To verify that all modern
299 contamination was removed, we ran *Schmutzi* again with the filtered reads. The depth of
300 coverage was then recorded using *Qualimap*.

301

302 *Uniparental Markers and sex Determination analyses*

303 The mtDNA haplogroup was determined using *SAMtools* pileup tool calling the positions defined
304 in the *Phylotree* database (42). We used a genome browser (*IGV*.v2.4.14) to study the genomic
305 context of each possible SNP (43). Only those SNPs that were present in two or more reads, and
306 those which were not located at the ends of the reads, were considered. The contamination was
307 estimated by calculating the ratio of discordant reads at haplogroup-diagnostic positions.
308 Molecular sex was assigned with *Ry_compute* (44), a script designed for the sex identification of
309 low coverage individuals (Fig. S1).

310

311 *Population Genetics Analysis*

312 A Principal Component Analysis (PCA) was performed using *SmartPCA* in *EIG* v6.0.1 with a subset
313 of modern individuals from the Human Origins dataset (45). This subset contained 434 present-
314 day Europeans and 616,938 autosomal SNPs, plus our sample. The Marat sample was projected
315 using the option *Isqproject*. As projected individuals' components tend to 0, we also carried out
316 a control analysis using Han Chinese, French and Marat (Fig. S3). The results were visualised
317 using the R package *GGplot2* (46). This dataset confirmed that Marat is not artefactually placed
318 at the centre of the plot.

319
320
321
322
323
324
325
326
327
328
329
330
331
332
333
334
335
336
337
338
339
340
341
342
343
344
345
346
347
348
349
350
351
352
353
354
355
356
357
358
359
360
361
362
363
364
365
366
367
368
369
370

We additionally ran an unsupervised clustering analysis using *ADMIXTURE* v1.3 and another subset of the Human Origins dataset (47). This subset included 881 individuals from Europe, West Asia and North Africa typed over 616,938 shared autosomal SNPs. We filtered the dataset by removing SNPs in high linkage disequilibrium using PLINK.v1.9 (48), removing all SNPs with a r^2 threshold of 0.4 within a 200 SNP sliding window, advancing by 50 SNPs each time. We performed the clustering analysis using K values ranging from 1 to 10, with 10 replicates for each value of K. We selected K according to the lowest cross-validation error value (K=4). The *ADMIXTURE* results at K=4 were visualised using the R package *pophelper* (49).

Metagenomic analysis

We first removed adapters and merged the paired-end reads into longer single-end sequences using AdapterRemoval v2 (50). We removed PCR duplicates with exact sequence identity using dedupe from the BBMap suite of tools (<https://sourceforge.net/projects/bbmap/>) (51). We subsequently used the default preprocessing pipeline designed for metaMix which consists of removing human and rRNA sequences using bowtie2 followed by megaBLAST, as well as low quality and low complexity reads using prinseq (52) (-lc_method dust -lc_threshold 7 -min_qual_mean 15). We then screened the remaining DNA reads for the presence of possible pathogens using both KrakenUniq (8) against the Kraken database compiled in Lassalle et al 2018 (53) and metaMix (7) using megaBLAST and a local custom database consisting of the RefSeq sequences of bacteria, viruses, parasites, fungi and human, as of July 2019. KrakenUniq was run with default parameters. The metaMix-nucleotide mode was run with the default number of 12 MCMC chains x 10,000 iterations and the default read support parameter of 10 reads was used.

The relative proportion of reads assigned to different species by KrakenUniq and metaMix was highly correlated; $R^2=0.94$ and $R^2=0.82$, for the blood stain and the unstained paper, respectively (Fig. S4). However, metaMix tended to assign a higher number of reads to individual species, closer to the number found by mapping directly to the microbial genomes and we observed important discrepancies for the number of reads assigned to some of the species (Table S4). Additionally, metaMix results for both the blood stain and the unstained paper consisted of fewer species compared to KrakenUniq, even when the same read support threshold was applied to KrakenUniq, indicating increased specificity due to the MCMC exploration of the species space, that comes at an increased computational cost.

In order to compare the accuracy of the two assignment tools, we further explored the presence of clinically relevant species by mapping the quality-filtered subset of reads (Table S4) used in metagenomic assignment against the reference genomes of different candidate genera of fungi and bacteria using *bowtie2* (33) and *BWA* v.07.3 (Fig. S5-S7, Fig. S9-S10). For all reads mapping to individual reference genomes, mapDamage v2 (35) was also run to assess evidence of nucleotide mis-incorporation characteristic of post-mortem damage. These mapping results were systematically supporting the metaMix assignments over those obtained with KrakenUniq (Table S4). This led us to rely on metaMix for all metagenomic assignments presented in the paper.

Besides testing for the presence and absence of species, we tested whether some microorganisms were overrepresented in the blood stain compared to the unstained section of the paper using a one-sided binomial test and a significance threshold of 0.95 (Table S3).

In the case of *Malassezia*, a phylogenetic analysis of the mitochondrial DNA genome with modern strains was performed. We called variant positions using *GATK UnifiedGenotyper* (54) and generated a Maximum Likelihood tree using *RAXML-NG* specifying a GTR substitution model and 100 bootstrap resamples (55). The tree was rooted with *M. globosa* (Fig. S8).

371

372 We also conducted a phylogenetic analysis for *C. acnes*, combining our historical strain with all
373 *C. acnes* genomes deposited in the Short Read Archive (SRA) covering the reference at an
374 average depth >10x, and with *C. namnetense* as an outgroup (SRR9222443). The only *C. acnes*
375 genomes sequenced at medium to high depth were those reported by Gomes et al 2017 (14). A
376 Maximum Likelihood tree was generated over the 21,751SNP alignment using RAxML-NG (Fig.
377 S11) and clonal complexes and phylotypes were assigned based on the PubMLST *C. acnes*
378 definitions database (https://pubmlst.org/bigsub?db=pubmlst_pacnes_seqdef).

379

380

381 **Acknowledgments**

382

383 This work was supported by Obra Social “La Caixa” and Secretaria d’Universitats i Recerca
384 (GRC2017-SGR880) (T.M.-B. and C.L.-F.), BFU2017-86471-P and PGC2018-101927-B-I00
385 (MINECO/FEDER, UE) (T.M.-B) and PGC2018-095931-B-100 (MINECO/FEDER, UE) (C.L.-F.). T.M.-
386 B. is also supported by a U01 MH106874 grant and Howard Hughes International Early Career
387 and CERCA Programme del Departament d’Economia i Coneixement de la Generalitat de
388 Catalunya. S.M is funded by a Wellcome Trust post-doctoral fellowship (206478/Z/17/Z). L.v.D
389 and F.B. acknowledge financial support from the Newton Fund UK-China NSFC initiative (grant
390 MR/P007597/1) and the BBSRC (equipment grant BB/R01356X/1).

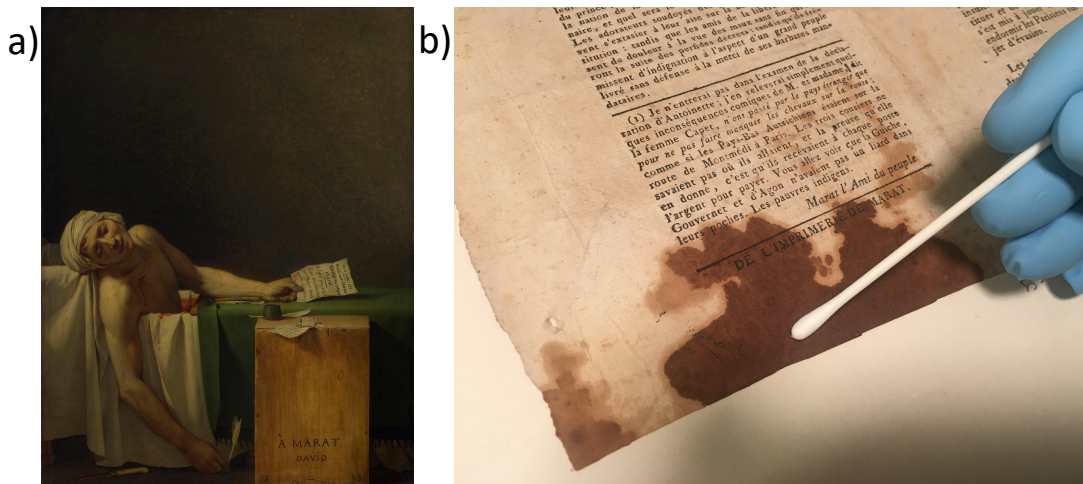
391 **References**

- 392
- 393 1. H. P. Bayon, The Medical Career of Jean-Paul Marat. *Proc. R. Soc. Med.* **39**, 39–44
- 394 (1945).
- 395 2. J. H. L. Cohen, E. L. Cohen, Doctor Marat and His Skin. *Med. Hist.* **2**, 281–286 (1958).
- 396 3. W. Dotz, Jean Paul Marat. His life, cutaneous disease, death, and depiction by Jacques
- 397 Louis David. *Am. J. Dermatopathol.* **1**, 247–250 (1979).
- 398 4. J. E. Jelinek, Jean-Paul Marat. The differential diagnosis of his skin disease. *Am. J.*
- 399 *Dermatopathol.* **1**, 251–252 (1979).
- 400 5. P. M. Dale, *Medical Biographies. The Ailments of Thirty-Three Famous Persons.*,
- 401 Norman, Ed. (Press, University of Oklahoma, 1952) <https://doi.org/10.1086/399828>.
- 402 6. C. Coto-Segura, P. Coto-Segura, J. Santos-Juanes, The Skin of a Revolutionary. *JAMA*
- 403 *Dermatology* **147**, 539 (2011).
- 404 7. S. Morfopoulou, V. Plagnol, Bayesian mixture analysis for metagenomic community
- 405 profiling. *Bioinformatics* **31**, 2930–2938 (2015).
- 406 8. F. P. Breitwieser, D. N. Baker, S. L. Salzberg, KrakenUniq: confident and fast
- 407 metagenomics classification using unique k-mer counts. *Genome Biol.* **19**, 198 (2018).
- 408 9. C. F. P. Scholz, M. Kilian, The natural history of cutaneous propionibacteria, and
- 409 reclassification of selected species within the genus *Propionibacterium* to the proposed
- 410 novel genera *Acidipropionibacterium* gen. nov., *Cutibacterium* gen. nov. and
- 411 *Pseudopropionibacterium* gen. nov. *Int. J. Syst. Evol. Microbiol.* **66**, 4422–4432 (2016).
- 412 10. B. Dreno, *et al.*, Skin microbiome and acne vulgaris: *Staphylococcus*, a new actor in
- 413 acne. *Exp. Dermatol.* **26**, 798–803 (2017).
- 414 11. S. J. Salter, *et al.*, Reagent and laboratory contamination can critically impact sequence-
- 415 based microbiome analyses. *BMC Biol.* **12**, 87 (2014).
- 416 12. S. Mollerup, *et al.*, *Propionibacterium acnes*: Disease-causing agent or common
- 417 contaminant? detection in diverse patient samples by next- generation sequencing. *J.*
- 418 *Clin. Microbiol.* **54**, 980–987 (2016).
- 419 13. E. Platsidaki, C. Dessinioti, Recent advances in understanding *Propionibacterium acnes* (
- 420 *Cutibacterium acnes*) in acne. *F1000Research* **7**, F1000 Faculty Rev-1953 (2018).
- 421 14. A. Gomes, *et al.*, Sonication of heart valves detects more bacteria in infective
- 422 endocarditis. *Sci. Rep.* **8**, 12967 (2018).
- 423 15. H. B. Lomholt, M. Kilian, Population Genetic Analysis of *Propionibacterium acnes*
- 424 Identifies a Subpopulation and Epidemic Clones Associated with Acne. *PLoS One* **5**,
- 425 e12277 (2010).
- 426 16. S. Nazipi, K. Stodkilde-Jorgensen, C. Scavenius, H. Bruggemann, The Skin Bacterium
- 427 *Propionibacterium acnes* Employs Two Variants of Hyaluronate Lyase with Distinct
- 428 Properties. *Microorganisms* **5** (2017).
- 429 17. P. Gelabert, *et al.*, Mitochondrial DNA from the eradicated European *Plasmodium vivax*
- 430 and *P. falciparum* from 70-year-old slides from the Ebro Delta in Spain . *Proc. Natl.*
- 431 *Acad. Sci.* **113**, 11495–11500 (2016).
- 432 18. S. Rasmussen, *et al.*, Early Divergent Strains of *Yersinia pestis* in Eurasia 5,000 Years
- 433 Ago. *Cell* **163**, 571–582 (2015).
- 434 19. N. Rascovan, *et al.*, Emergence and Spread of Basal Lineages of *Yersinia pestis* during
- 435 the Neolithic Decline. *Cell* **176**, 295–305.e10 (2019).
- 436 20. A. Margaryan, *et al.*, Ancient pathogen DNA in human teeth and petrous bones. *Ecol.*
- 437 *Evol.* **8**, 3534–3542 (2018).
- 438 21. B. Mühlemann, *et al.*, Ancient hepatitis B viruses from the Bronze Age to the Medieval
- 439 period. *Nature* **557**, 418–423 (2018).
- 440 22. S. Marciniak, *et al.*, *Plasmodium falciparum* malaria in 1st–2nd century CE southern
- 441 Italy. *Curr. Biol.* **26**, R1220–R1222 (2016).
- 442 23. A. M. Devault, *et al.*, Second-Pandemic Strain of *Vibrio cholerae* from the Philadelphia

- 443 Cholera Outbreak of 1849 . *N. Engl. J. Med.* **370**, 334–340 (2014).
- 444 24. T. de-Dios, *et al.*, Genetic affinities of an eradicated European Plasmodium falciparum
445 strain. *Microb. genomics* **5** (2019).
- 446 25. T. E. King, *et al.*, Identification of the remains of King Richard III. *Nat. Commun.* **5**, 5631
447 (2014).
- 448 26. I. Olalde, *et al.*, Genomic analysis of the blood attributed to Louis XVI (1754–1793), king
449 of France. *Sci. Rep.* **4**, 4666 (2014).
- 450 27. C. W. Saunders, A. Scheynius, J. Heitman, Malassezia Fungi Are Specialized to Live on
451 Skin and Associated with Dandruff, Eczema, and Other Skin Diseases. *PLOS Pathog.* **8**,
452 e1002701 (2012).
- 453 28. R. Ashbee, E. Bignell, Eds., “Pathogenic yeasts” in *The Yeast Handbook*, (Springer-
454 Verlag, 2010), pp. 209–230.
- 455 29. A. K. Gupta, R. Batra, R. Bluhm, T. Boekhout, T. L. Dawson, Skin diseases associated with
456 Malassezia species. *J. Am. Acad. Dermatol.* **51**, 785–798 (2004).
- 457 30. C. Carøe, *et al.*, Single-tube library preparation for degraded DNA. *Methods Ecol. Evol.*
458 **9**, 410–419 (2018).
- 459 31. M. Martin, Cutadapt removes adapter sequences from high-throughput sequencing
460 reads. *EMBnet.journal* **17**, 10–12 (2011).
- 461 32. H. Li, R. Durbin, Fast and accurate short read alignment with Burrows-Wheeler
462 transform. *Bioinformatics* **25**, 1754–1760 (2009).
- 463 33. B. Langmead, S. L. Salzberg, Fast gapped-read alignment with Bowtie 2. *Nat. Methods* **9**,
464 357–359 (2012).
- 465 34. Broad Institute, Picard.
- 466 35. H. Jónsson, *et al.*, mapDamage2.0: fast approximate Bayesian estimates of ancient DNA
467 damage parameters. in *Bioinformatics*, (2013), pp. 1682–1684.
- 468 36. F. García-Alcalde, *et al.*, Qualimap: Evaluating next-generation sequencing alignment
469 data. *Bioinformatics* **28**, 2678–2679 (2012).
- 470 37. H. Li, *et al.*, The Sequence Alignment/Map format and SAMtools. *Bioinformatics* **25**,
471 2078–2079 (2009).
- 472 38. I. Lazaridis, *et al.*, Ancient human genomes suggest three ancestral populations for
473 present-day Europeans. *Nature* **513**, 409–413 (2014).
- 474 39. I. Lazaridis, *et al.*, Genotypes of ancient individuals and fully public Affymetrix Human
475 Origins present-day individuals. *Genomic insights into Orig. farming Anc. Near East*
476 (2016).
- 477 40. G. Renaud, V. Slon, A. T. Duggan, J. Kelso, Schmutzi: Estimation of contamination and
478 endogenous mitochondrial consensus calling for ancient DNA. *Genome Biol.* **16**, 1–18
479 (2015).
- 480 41. L. Pierre, Jvarkit: java-based utilities for Bioinformatics. *Figshare* (2015)
481 <https://doi.org/10.6084/m9.figshare.1425030.v1>.
- 482 42. M. van Oven, PhyloTree Build 17: Growing the human mitochondrial DNA tree. *Forensic*
483 *Sci. Int. Genet. Suppl. Ser.* **5**, e392–e394 (2015).
- 484 43. J. T. Robinson, *et al.*, Integrative genomics viewer. *Nat. Biotechnol.* **29**, 24–26 (2011).
- 485 44. P. Skoglund, J. Storå, A. Götherström, M. Jakobsson, Accurate sex identification of
486 ancient human remains using DNA shotgun sequencing. *J. Archaeol. Sci.* **40**, 4477–4482
487 (2013).
- 488 45. N. Patterson, A. L. Price, D. Reich, Population structure and eigenanalysis. *PLoS Genet.*
489 **2**, e190 (2006).
- 490 46. H. Wickham, *ggplot2: Elegant Graphics for Data Analysis* (Springer-Verlag New York,
491 2016).
- 492 47. D. H. Alexander, J. Novembre, K. Lange, Fast model-based estimation of ancestry in
493 unrelated individuals. *Genome Res.* **19**, 1655–64 (2009).
- 494 48. S. Purcell, *et al.*, PLINK: A Tool Set for Whole-Genome Association and Population-Based

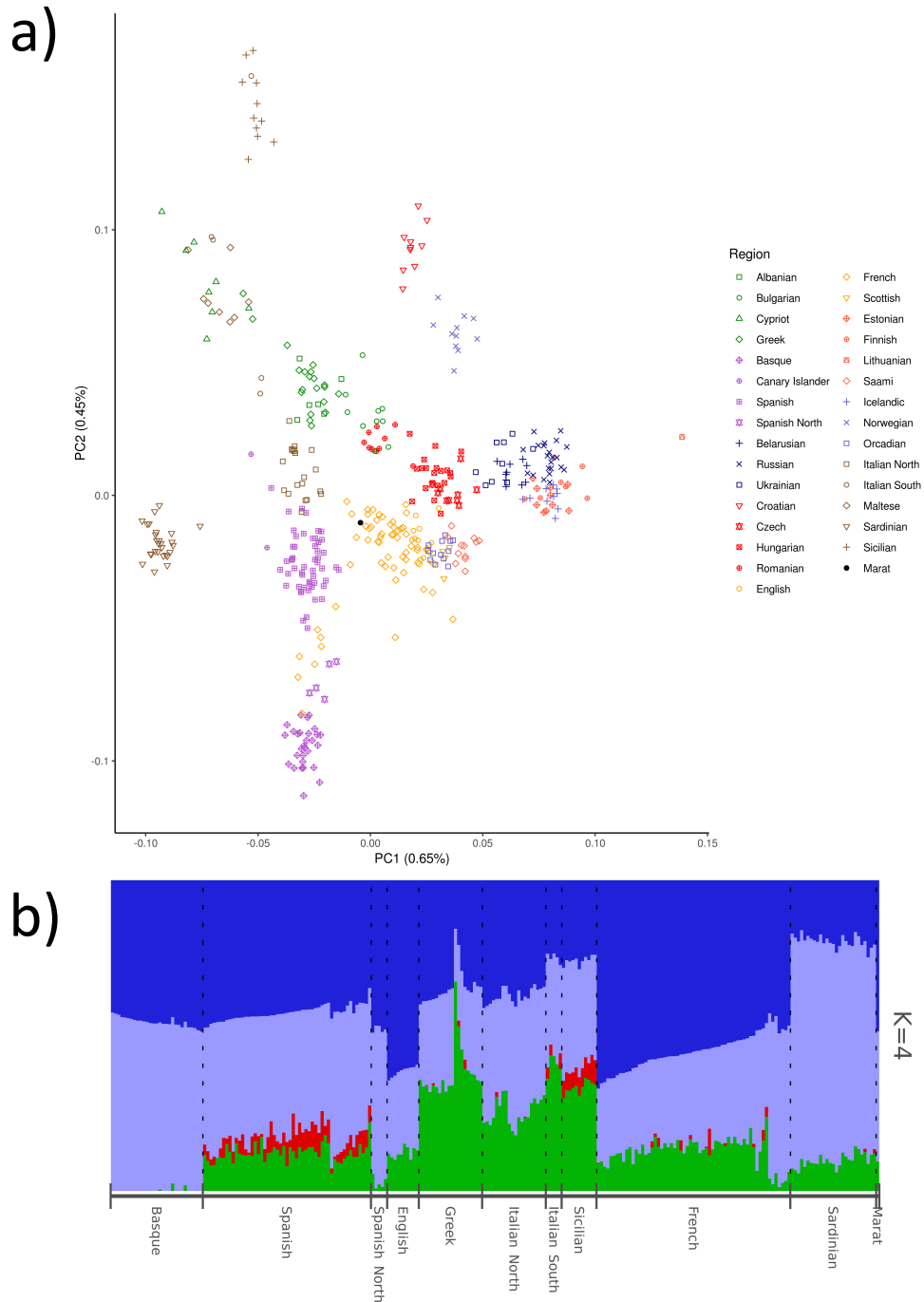
- 495 Linkage Analyses. *Am. J. Hum. Genet.* **81**, 559–575 (2007).
496 49. R. M. Francis, pophelper: an R package and web app to analyse and visualize population
497 structure. *Mol. Ecol. Resour.* **17**, 27–32 (2017).
498 50. M. Schubert, S. Lindgreen, L. Orlando, AdapterRemoval v2: rapid adapter trimming,
499 identification, and read merging. *BMC Res. Notes* **9**, 88 (2016).
500 51. B. B., BMap (2014).
501 52. R. Schmieder, R. Edwards, Quality control and preprocessing of metagenomic datasets.
502 *Bioinformatics* **27**, 863–864 (2011).
503 53. F. Lassalle, *et al.*, Oral microbiomes from hunter-gatherers and traditional farmers
504 reveal shifts in commensal balance and pathogen load linked to diet. *Mol. Ecol.* **27**,
505 182–195 (2018).
506 54. M. D. McKenna, Aaron, Matthew Hanna, Eric Banks, Andrey Sivachenko, Kristian
507 Cibulskis, Andrew Kernytsky, Kiran Garimella, David Altshuler, Stacey Gabriel, *et al.*, The
508 Genome Analysis Toolkit: A MapReduce framework for analyzing next-generation DNA
509 sequencing data. *Genome Res.* **20**, 254–260 (2010).
510 55. A. M. Kozlov, D. Darriba, T. Flouri, B. Morel, A. Stamatakis, RAxML-NG: a fast, scalable
511 and user-friendly tool for maximum likelihood phylogenetic inference. *Bioinformatics*
512 (2019) <https://doi.org/10.1093/bioinformatics/btz305>.
513

514 **Figures and Tables**
515



516
517

518 **Figure 1:** a) "La mort de Marat"; portrait of Jean-Paul Marat after his assassination, by Jacques-
519 Louis David (1793). Preserved at Musées Royaux des Beaux-Arts de Belgique, Brussels. b)
520 Sampling the page of *l'Ami du Peuple* stained with Marat's blood that has been analysed.



521
 522 **Figure 2:** a) Principal Component Analysis (PCA) of modern human European populations with
 523 Marat's ancient DNA reads projected on it. b) Admixture analysis with modern European
 524 samples and Marat. Both analyses are coherent with Marat's suggested French and Italian
 525 combined ancestry.

Table 1: List of diseases tested for associated agents and presence in the blood stain and the unstained paper samples. The following symbols denote the abundance of reads for each infectious agent tested. ✓: present; ✓✓: top ten; ✓✓✓: top hit; ✗: absent.

Disease	Pathogen	Blood	Unstained paper
Syphilis	<i>Treponema pallidum</i>	✗	✗
Scrofula (tuberculosis)	<i>Mycobacterium tuberculosis</i> ¹	✗	✗
Leprosy	<i>Mycobacterium leprae</i>	✗	✗
Diabetic candidiasis (thrush)	<i>Candida</i> sp.	✗	✗
Scabies	<i>Sarcoptes scabiei</i>	✗	✗
Seborrheic dermatitis	<i>Malassezia</i> sp.	✓✓	✓
Atopic eczema	<i>Staphylococcus aureus</i>	✓	✗
Severe acneiform eruptions	<i>Cutibacterium acnes</i>	✓✓✓	✓✓

¹ Scrofula can also be caused by other Mycobacteria in particular *M. scrofulaceum* and *M. avium intracellulare*, which are also absent from both samples.